Effect of elevated pCO_2 on trace gas production during an ocean acidification mesocosm experiment

Sheng-Hui Zhang[1,3§], Juan Yu[1,2§], Qiong-Yao Ding[1], Gui-Peng Yang[1,2*], Kun-Shan Gao[4], Hong-Hai Zhang[1,2], Da-Wei Pan[3]

[1] Key Laboratory of Marine Chemistry Theory and Technology, Ministry of Education, Ocean University of China, Qingdao 266100, China;

[2] Laboratory for Marine Ecology and Environmental Science, Qingdao National Laboratory for Marine Science and Technology, Qingdao 266237, China

[3] Key Laboratory of Coastal Environmental Processes and Ecological Remediation, Yantai Institute of Coastal Zone Research (YIC), Chinese Academy of Sciences(CAS); Shandong Provincial Key Laboratory of Coastal Environmental Processes, YICCAS, Yantai Shandong 264003, P. R. China

[4] State Key Laboratory of Marine Environmental Science, Xiamen University, Xiamen, 361102, China

* Corresponding author:
Prof. Gui-Peng Yang
Key Laboratory of Marine Chemistry Theory and Technology
Ocean University of China
Qingdao 266100
China
E-mail: gpyang@mail.ouc.edu.cn
Tel: +86-532-66782657
Fax: +86-532-66782657

Author contributions
[§]Sheng-Hui Zhang and JuanYu contributed equally

Abstract

A mesocosm experiment was conducted in Wuyuan Bay (Xiamen), China to investigate the effects of elevated pCO_2 on the phytoplankton species *Phaeodactylum tricornutum* (*P. tricornutum*), *Thalassiosira weissflogii* (*T. weissflogii*) and *Emiliania huxleyi* (*E. huxleyi*) and their production ability of dimethylsulfide (DMS), dimethylsulfoniopropionate (DMSP), as well as four halocarbon compounds bromodichloromethane ($CHBrCl_2$), methyl bromide (CH_3Br), dibromomethane (CH_2Br_2) and iodomethane (CH_3I). Over a period of 5 weeks, *P. tricornuntum* outcompeted *T. weissflogii* and *E. huxleyi*, comprising more than 99% of the final biomass. During the logarithmic growth phase (phase I), mean DMS concentration in high pCO_2 mesocosms (1000 μatm) was 28% lower than that in low pCO_2 mesocosms (400 μatm). Elevated pCO_2 led to a delay in DMSP-consuming bacteria concentrations attached to *T. weissflogii* and *P. tricornutum* and finally resulted in the delay of DMS concentration in the high pCO_2 treatment. Unlike DMS, the elevated pCO_2 did not affect DMSP production ability of *T. weissflogii* or *P. tricornuntum* throughout the 5 weeks culture. A positive relationship was detected between CH_3I and *T. weissflogii* and *P. tricornuntum* during the experiment, and there was a 40% reduction in mean CH_3I concentration in the high pCO_2 mesocosms. $CHBrCl_2$, CH_3Br, and CH_2Br_2 concentrations did not increase with elevated chlorophyll a (Chl *a*) concentrations compared with DMS(P) and CH_3I, and there were no major peaks both in the high pCO_2 or low pCO_2 mesocosms. In addition, no effect of elevated pCO_2 was identified for any of the three bromocarbons.

Keywords: ocean acidification, dimethylsulfide (DMS), dimethylsulfoniopropionate (DMSP), halocarbons, phytoplankton, bacteria

1. Introduction

Anthropogenic emissions have increased the fugacity of atmospheric carbon dioxide (pCO_2) from the pre-industrial value of 280 µatm to the present-day value of over 400 µatm, and these values will further increase to 800–1000 µatm by the end of this century (Gattuso et al., 2015). The dissolution of this excess CO_2 into the surface of the ocean directly affects the carbonate system and has lowered the pH by 0.1 units, from 8.21 to 8.10 over the last 250 years. Further decreases of 0.3–0.4 pH units are predicted by the end of this century (Doney et al., 2009; Orr et al., 2005; Gattuso et al., 2015), which is commonly referred to as ocean acidification. The physiological and ecological aspects of the phytoplankton response to this changing environment can potentially alter marine phytoplankton community composition, community biomass, and feedback to biogeochemical cycles (Boyd and Doney, 2002). These changes simultaneously have an impact on some volatile organic compounds produced by marine phytoplankton (Liss et al., 2014; Liu et al., 2017), including the climatically important trace gas dimethylsulfide (DMS) and a number of volatile halocarbon compounds.

DMS is the most important volatile sulfur compound produced from dimethylsulfoniopropionate (DMSP), which is ubiquitous in marine environments, mainly synthesized by marine microalgae (Stefels et al., 2007), a few angiosperms, some corals (Raina et al., 2016), and several heterotrophic bacteria (Curson et al., 2017) through complex biological interactions in marine ecosystems. Although it remains controversial, DMS and its by-products, such as methanesulfonic acid and non-sea-salt sulfate, are suspected to have a prominent part in climate feedback (Charlson et al., 1987; Quinn and Bates, 2011). The conversion of DMSP to DMS is facilitated by several enzymes, including DMSP-lyase and acyl CoA transferase

70 (Kirkwood et al., 2010; Todd et al., 2007); these enzymes are mainly found in phytoplankton,
71 macroalgae, symbiodinium, bacteria and fungi (de Souza and Yoch, 1995; Stefels and Dijkhuizen,
72 1996; Steinke and Kirst, 1996; Bacic and Yoch, 1998; Yost and Mitchelmore, 2009). Several
73 studies have shown a negative impact of decreasing pH on DMS-production capability (Hopkins
74 et al., 2010; Avgoustidi et al., 2012; Archer et al., 2013; Webb et al., 2016), while others have
75 found either no effect or a positive effect (Vogt et al., 2008; Hopkins and Archer, 2014). Several
76 assumptions have been presented to explain these contrasting results and attributed the
77 pH-induced variation in DMS-production capability to altered physiology of the algae cells or of
78 bacterial DMSP degradation (Vogt et al., 2008; Hopkins et al., 2010, Avgoustidi et al., 2012;
79 Archer et al., 2013; Hopkins and Archer, 2014; Webb et al., 2015).
80 Halocarbons also play a significant role in the global climate because they are linked to
81 tropospheric and stratospheric ozone depletion and a synergistic effect of chlorine and bromine
82 species has been reported accounting for approximately 20% of the polar stratospheric ozone
83 depletion (Roy et al., 2011). In addition, iodocarbons can release atomic iodine quickly through
84 photolysis in the atmospheric boundary layer and iodine atoms are very efficient in the catalytic
85 removal of O_3, which governs the lifetime of many climate relevant gases including methane and
86 DMS (Jenkins et al., 1991). Compared with DMS, limited attention was received about the effect
87 of ocean acidification on halocarbon concentrations. Hopkins et al. (2010) and Webb et al. (2015)
88 measured lower concentrations of several iodocarbons, while bromocarbons were unaffected by
89 elevated pCO_2 in two acidification experiments. In addition, another mesocosm study did not elicit
90 significant differences from any halocarbon compounds at up to 1,400 µatm pCO_2 (Hopkins et al.,
91 2013).

92 Taken together, the data indicate that the response of DMS and halocarbon release to elevated
93 pCO_2 is complex and controversial. DMS and halocarbons play a significant role in the global
94 climate and will perhaps act to a greater extent in the future. An intermediate step between
95 laboratory and natural community field experiments was designed in this study to understand the
96 response of the release of DMS and halocarbon to ocean acidification in Chinese coastal seas
97 using isolates of non-axenic phytoplankton added to filtered natural water. We hypothesized that
98 the response of DMS and halocarbon release to elevated pCO_2 in natural seawater can be better
99 presented after minimizing the shifting composition of the natural phytoplankton and microbial
100 communities.

101 **2. Experimental method**

102 *2.1 Experimental setup*

103 To investigate the response of DMS and halocarbon release to ocean acidification, a mesocosm
104 experiment was carried out on a floating platform (set in seawater, about 150 m from the shore) at
105 the Facility for Ocean Acidification Impacts Study of Xiamen University (FOANIC-XMU,
106 24.52 °N, 117.18 °E) (for full technical details of the mesocosms, see Liu et al. 2017). Six
107 cylindrical transparent thermoplastic polyurethane bags with domes were deployed along the
108 south side of the platform. The width and depth of each mesocosm bag was 1.5 m and 3 m,
109 respectively. Filtered (0.01 μm ultrafiltration water purifier, MU801-4T, Midea, Guangdong,
110 China) in situ seawater was pumped into the six bags simultaneously within 24 hrs. A known
111 amount of NaCl solution was added to each bag to calculate the exact volume of seawater in the
112 bags, according to a comparison of the salinity before and after adding salt (Czerny et al., 2013).
113 The initial in situ pCO_2 was about 650 μatm. To set the low (400 μatm) and high pCO_2 (1000 μatm)

levels, we added Na_2CO_3 solution and CO_2 saturated seawater to the mesocosm bags to alter total alkalinity and dissolved inorganic carbon (Gattuso et al., 2010; Riebesell et al., 2013). Subsequently, during the whole experimental process, air at the ambient (400 μatm) and elevated pCO_2 (1000 μatm) concentrations was continuously bubbled into the mesocosm bags using a CO_2 Enricher (CE-100B, Wuhan Ruihua Instrument & Equipment Ltd., Wuhan, China). Seawater taken from the coastal environment was first filtered to remove algae and their attached bacteria before usage in mesocosm bags. Bacterial abundance in the pre-filtered water was less than 10^3 cell mL^{-1}, which was three magnitudes lower than the bacterial abundance in the natural water and close to the detection limit of the flow cytometer. The trace gases, including DMS, bromodichloromethane ($CHBrCl_2$), methyl bromide (CH_3Br), dibromomethane (CH_2Br_2), and iodomethane (CH_3I) produced in the environment did not affect the mesocosm trace gas concentrations after the bags were sealed.

2.2 Algal strains

Before being introduced into the mesocosms, the three phytoplankton species *Phaeodactylum tricornutum* (*P. tricornutum*), *Thalassiosira weissflogii* (*T. weissflogii*) and *Emiliania huxleyi* (*E. huxleyi*) were cultured in autoclaved, pre-filtered seawater from Wuyuan Bay at 16 ℃ (similar to the in situ temperature of Wuyuan Bay) without any addition of nutrients. Cultures were continuously aerated with filtered ambient air containing 400 μatm of CO_2 within plant chambers (HP1000G-D, Wuhan Ruihua Instrument & Equipment, China) at a constant bubbling rate of 300 mL min^{-1}. The culture medium was renewed every 24 hrs to maintain the cells of each phytoplankton species in exponential growth. When the experiment began, these three phytoplankton species were inoculated into the mesocosm bags, with an initial

diatom/coccolithophorid cell ratio of 1:1. The initial concentrations of *P. tricornuntum*, *T. weissflogii*, and *E. huxleyi* inoculated into the mesocosm were 10, 10, and 20 cells mL^{-1}, respectively. *P. tricornuntum* and *T. weissflogii* were obtained from the Center for Collections of Marine Bacteria and Phytoplankton of the State Key Laboratory of Marine Environmental Science (Xiamen University). *P. tricornuntum* was originally isolated from the South China Sea in 2004 and *T. weissflogii* was isolated from Daya Bay in the coastal South China Sea. *E. huxleyi* was originally isolated in 1992 from the field station of the University of Bergen (Raunefjorden; 60°18'N, 05°15'E).

2.3 Sampling for DMS(P) and halocarbons

DMS(P) and halocarbon samples were taken from the above mentioned mesocosm bags at 9 a.m., then all collected samples were transported into a dark cool box back to the laboratory onshore for analysis within 1 hr. For the DMS analysis, 2 mL sample was gently filtered through a 25 mm GF/F (glass fiber) filter and transferred to a purge and trap system linked to a Shimadzu GC-2014 gas chromatograph (Tokyo, Japan) equipped with a glass column packed with 10% DEGS on Chromosorb W-AW-DMCS (3 m × 3 mm) and a flame photometric detector (Zhang et al., 2014). For total DMSP analysis, 10 mL water sample was fixed using 50 μL of 50 % H_2SO_4 and sealed (Kiene and Slezak, 2006). After > 1 d preservation, DMSP samples were hydrolyzed for 24 hrs with a pellet of KOH (final pH > 13) to fully convert DMSP to DMS. Then, 2 mL of the hydrolyzed sample was carefully transferred to the purge and trap system mentioned above for extraction of DMS. For halocarbons, 100 mL sample was purged at 40 ℃ with pure nitrogen at a flow rate of 100 mL min^{-1} for 12 min using another purge and trap system coupled to an Agilent 6890 gas chromatograph (Agilent Technologies, Palo Alto, CA, USA) equipped with an electron

158 capture detector (ECD) as well as a 60 m DB-624 capillary column (0.53 mm ID; film thickness, 3
159 μm) (Yang et al., 2010). The analytical precision for duplicate measurements of DMS(P) and
160 halocarbons was > 10%.

161 *2.4 Measurements of chlorophyll a*

162 Chlorophyll *a* (Chl *a*) was measured in water samples (200–1,000 mL) collected every 2 d at 9
163 a.m. by filtering onto Whatman GF/F filters (25 mm). The filters were placed in 5 mL 100%
164 methanol overnight at 4 ℃ and centrifuged at 5000 r min^{-1} for 10 min. The absorbance of the
165 supernatant (2.5 mL) was measured from 250 to 800 nm using a scanning spectrophotometer (DU
166 800, Beckman Coulter Inc., Brea, CA, USA). Chl *a* concentration was calculated according to the
167 equation reported by Porra (2002).

168 *2.5 Enumeration of DMSP-consuming bacteria*

169 The number of DMSP-consuming bacteria in the mesocosms was estimated using the most
170 probable number methodology. The medium consisted of a mixture (1:1 v/v) of sterile artificial
171 sea water and mineral medium (Visscher et al., 1991), 3 mL of which was dispensed into 6 mL test
172 tubes, which were closed by an over-sized cap, allowing gas exchange. Triplicate dilution series
173 were set up. All test tubes contained 1 mmol L^{-1} DMSP as the sole organic carbon source and
174 were kept at 30 ℃ in the dark. After 2 weeks, the presence/absence of bacteria in the tubes was
175 verified by DAPI staining (Porter and Feig, 1980). Three tubes containing 3 mL ASW without
176 substrate were used as controls.

177 *2.6 Statistical analysis*

178 One-way analysis of variance (ANOVA), Tukey's test, and the two-sample t-test were carried out
179 to demonstrate the differences between treatments. A p-value < 0.05 was considered significant.

Relationships between DMS(P), halocarbons and a range of other parameters were detected using Pearson's correlation analysis via SPSS 22.0 for Windows (SPSS Inc., Chicago, IL, USA).

3. Results and Discussion

3.1 Temporal changes in pH, Chl a, P. tricornuntum, T. weissflogii, and E. huxleyi during the experiment

During the experiment, the seawater in each mesocosm was well mixed, and the temperature and salinity remained stable, with means of 16 ℃ and 29, respectively, in all mesocosm bags. We observed significant differences in pH levels between the two CO_2 treatments on days 0–11, but the differences disappeared with subsequent phytoplankton growth (Fig. 1). The phytoplankton growth process was divided into three phases in terms of variations in Chl *a* concentrations in the mesocosm experiments as described in Liu et al. (2017): i) the logarithmic growth phase (phase I, days 0–13), ii) a plateau phase (phase II, days 13–23, bloom period), and iii) a secondary plateau phase (phase III, days 23–33) attained after a decline in biomass from a maximum in phase II. The initial chemical parameters of the mesocosm experiment are shown in Table 1. The initial mean dissolved nitrate (including NO_3^- and NO_2^-), NH_4^+, PO_4^{3-} and silicate (SiO_3^{2-}) concentrations were 54, 20, 2.6 and 41 μmol L^{-1}, respectively for the low pCO_2 treatment and 52, 21, 2.4 and 38 μmol L^{-1}, respectively for the high pCO_2 treatment. The nutrient concentrations (NO_3^-, NO_2^-, NH_4^+ and phosphate) during phase I were consumed rapidly and their concentrations were below or close to the detection limit during phase II (Table 1). SiO_3^{2-} was detectable during the entire experimental period, and was unlikely to be a limiting factor for phytoplankton growth during the experiment. In addition, although dissolved inorganic nitrogen (NH_4^+, NO_3^-, and NO_2^-) and phosphate were depleted, Chl *a* concentration in both treatments (biomass dominated by *P.*

202 *tricornuntum*) remained constant over days 12–22, and then declined over subsequent days. *T.*
203 *weissflogii* was found throughout the entire period in each bag, but the maximum concentration
204 was 8,120 cells mL^{-1}, which was far less than the concentration of *P. tricornutum* with a
205 maximum density of about 1.5 million cells mL^{-1} (Liu et al., 2017). It is possible that *P.*
206 *tricornutum* outcompeted *T. weissflogii* because of its higher surface to volume ratio and/or
207 species-specific physiology, which would enhance the efficiency of nutrient uptake and related
208 metabolism (Alessandrade et al., 2007). *E. huxleyi* was only found in phase I and its maximal
209 concentration reached 310 cells mL^{-1} according to the results of Liu et al. (2017). Previous studies
210 have reported that the maximum specific growth rate of *T. weissflogii* and *P. tricornutum* is about
211 1.2 d^{-1} (Li et al., 2014; Sugie and Yoshimura, 2016), while that of *E. huxleyi* is about 0.8 d^{-1} (Xing
212 et al., 2015). This might be the main reason why diatoms overwhelmingly outcompeted the
213 coccolithophores during this experiment.

214 *3.2 Impact of elevated pCO_2 on DMS and DMSP production*

215 DMSP concentrations in the high pCO_2 and low pCO_2 treatments increased significantly along
216 with the increase in Chl *a* concentrations and algal cells, and remained relatively constant over the
217 following days. A significant positive relationship was observed between DMSP and
218 phytoplankton in the experiment ($r = 0.961$, $p < 0.01$ for *P. tricornuntum*, $r = 0.617$, $p < 0.01$ for *T.*
219 *weissflogii* in the low pCO_2 treatment, Table 2; $r = 0.954$, $p < 0.01$ for *P. tricornuntum*, $r = 0.743$, p
220 < 0.01 for *T. weissflogii* in the high pCO_2 treatment, Table 3). DMS was maintained at a low level
221 during phase I (mean of 1.03 nmol L^{-1} in the low pCO_2 and 0.74 nmol L^{-1} in the high pCO_2
222 treatments, respectively) compared with DMSP. DMS concentrations began to increase rapidly on
223 day 15, peaked on day 25 in the low pCO_2 treatment (112.1 nmol L^{-1}) and on day 29 in the high

224 pCO_2 treatment (101.9 nmol L^{-1}) respectively, and then decreased in the following days. A
225 moderate positive relationship was observed between DMS and *P. tricornuntum* (r = 0.560, $p <$
226 0.05 in the low pCO_2 treatment; r = 0.635, $p < 0.01$ in the high pCO_2 treatment), while no
227 relationship was observed between DMS and *T. weissflogii* (Table 2 and Table 3) during the
228 experiment. Similar to DMS, DMSP-consuming bacteria also maintained a low level during phase
229 I (mean of 0.57×10^6 and 0.40×10^6 cells mL^{-1} in the low pCO_2 and high pCO_2 treatments,
230 respectively). DMSP-consuming bacterial concentrations respectively peaked on days 19 ($11.65 \times$
231 10^6 cells mL^{-1}) and 21 (10.70×10^6 cells mL^{-1}) in the low pCO_2 and high pCO_2 treatments.
232 In this study, no difference in mean DMSP concentrations was observed between the two
233 treatments, indicating that elevated pCO_2 had no significant influence on DMSP production in *P.*
234 *tricornuntum* and *T. weissflogii*. However, significant reductions in mean DMS concentration
235 (28%) and DMSP-consuming bacteria (29%) were detected during phase I in the high pCO_2
236 treatment compared with those in the low pCO_2 treatment, indicating that elevated pCO_2 inhibited
237 DMSP-consuming bacteria and DMS production during the logarithmic growth phase. In addition,
238 the peak DMS concentration in the high pCO_2 treatment was delayed 4 days relative to that in the
239 low pCO_2 treatment during phase II (Fig. 2-A). This result has been observed in previous
240 mesocosm experiments and it was attributed to small scale shifts in community composition and
241 succession (Vogt et al., 2008; Webb et al., 2016). However, this phenomenon during the present
242 study can be explained in another straightforward way. Previous studies have shown that marine
243 bacteria play a key role in DMS production, and that the efficiency of bacteria converting DMSP
244 to DMS may vary from 2 to 100% depending on the nutrient status of the bacteria and the quantity
245 of dissolved organic matter (Simó et al., 2002, 2009; Kiene et al., 1999, 2000). In addition, a

246 significant positive relationship was observed between DMS and DMSP-consuming bacteria (r =
247 0.643, $p < 0.01$ in the low pCO_2 treatment; r = 0.544, $p < 0.01$ in the high pCO_2 treatment) during
248 this experiment. All of these observations point to the importance of bacteria in DMS and DMSP
249 dynamics. During the present mesocosm experiment, DMSP concentrations in the low pCO_2
250 treatment decreased slightly on day 23, while the slight decrease appeared on day 29 in the high
251 pCO_2 treatment (Fig. 2-B). In addition, the time that the DMSP concentration began to decrease
252 was very close to the time when the highest DMS concentration occurred in both treatments.
253 Similar to DMS, DMSP-consuming bacteria was also delayed in the high pCO_2 mesocosm
254 compared to that in the low pCO_2 mesocosm (Fig. 2-C). Taken together, we inferred that the
255 elevated pCO_2 first delayed growth of DMSP-consuming bacteria, then the delayed
256 DMSP-consuming bacteria postponed the DMSP degradation process, and eventually delayed the
257 DMS concentration in the high pCO_2 treatment. In addition, considering that algae and bacteria in
258 natural seawater were removed through a filtering process before the experiment (Huang et al.,
259 2018), we further concluded that the elevated pCO_2 controlled DMS concentrations mainly by
260 affecting DMSP-consuming bacteria attached to *T. weissflogii* and *P. tricornuntum*.

261 *3.3 Impact of elevated pCO_2 on halocarbon compounds*

262 The temporal development in $CHBrCl_2$, CH_3Br, and CH_2Br_2 concentrations is shown in Fig. 3-A,
263 Fig. 3-B, and Fig. 3-C, respectively. The temporal changes of their concentrations were
264 substantially different from those of DMS, DMSP, *P. tricornuntum* and *T. weissflogii*. The mean
265 concentrations of $CHBrCl_2$, CH_3Br, and CH_2Br_2 for the entire experiment were 8.58, 7.85, and
266 5.13 pmol L^{-1} in the low pCO_2 treatment and 8.81, 9.73, and 6.27 pmol L^{-1} in the high pCO_2
267 treatment. The concentrations of $CHBrCl_2$, CH_3Br, and CH_2Br_2 did not increase with the Chl *a*

concentration compared with those of DMS and DMSP, and no major peaks were detected in the mesocosms. In addition, no effect of elevated pCO_2 was identified for any of the three bromocarbons, which compared well with previous mesocosm findings (Hopkins et al., 2010, 2013; Webb et al., 2016). No clear correlation was observed between the three bromocarbons and any of the measured algal groups (table 2 and table 3), indicating that *P. tricornuntum* and *T. weissflogii* did not primarily release these three bromocarbons during the mesocosm experiment. Previous studies reported that large-size cyanobacteria, such as *Aphanizomenon flos-aquae*, could produce bromocarbons (Karlsson et al., 2008). Significant correlations between the abundance of cyanobacteria and several bromocarbons have been reported in the Arabian Sea (Roy et al., 2011). However, the filtration procedure led to the loss of cyanobacteria in the mesocosms and finally resulted in low bromocarbon concentrations during the experiment, although *P. tricornuntum* and *T. weissflogii* abundances were high.

The temporal dynamics of CH_3I in the high pCO_2 and low pCO_2 treatments are shown in Fig. 3-D. The CH_3I concentrations in the low pCO_2 treatment varied from 0.38 to 12.61 pmol L^{-1}, with a mean of 4.76 pmol L^{-1}. The CH_3I concentrations in the high pCO_2 treatment ranged between 0.44 and 8.78 pmol L^{-1}, with a mean of 2.88 pmol L^{-1}. The maximum CH_3I concentrations in the high pCO_2 and low pCO_2 treatments were both observed on day 23. The range of CH_3I concentrations during this experiment was similar to that measured in the mesocosm experiment (< 1~10 pmol L^{-1}) in Kongsfjorden conducted by Hopkins et al. (2013). In addition, the mean CH_3I concentration in the low pCO_2 treatment was similar to that measured in the East China Sea, with an average of 5.34 pmol L^{-1} in winter and 5.74 pmol L^{-1} in summer (Yuan et al., 2016). Meanwhile, a positive relationship was detected between CH_3I and Chl *a*, *P. tricornuntum* and *T.*

290 *weissflogii* (r = 0.588, $p < 0.01$ in the low pCO_2 treatment; r = 0.834, $p < 0.01$ in the low pCO_2
291 treatment for *P. tricornuntum*; r = 0.680, $p < 0.01$ in the low pCO_2 treatment; r = 0.690, $p < 0.01$
292 in the high pCO_2 treatment for *Thalassiosira weissflogii*; r = 0.717, $p < 0.01$ in the low pCO_2
293 treatment; r = 0.741, $p < 0.01$ in the high pCO_2 treatment for Chl *a*). This result agrees with
294 previous mesocosm (Hopkins et al., 2013) and laboratory experiments (Hughes et al., 2013;
295 Manley and De La Cuesta, 1997) identifying diatoms as significant producers of CH_3I. Moreover,
296 similar to DMS, the maximum CH_3I concentration also occurred after the maxima of *P.*
297 *tricornuntum* and *T. weissflogii*, at about 4 d (Fig. 3-D). This result was similar to the conclusions
298 reported by Hopkins et al. (2010) and Wingenter et al. (2007) during two mesocosm experiments
299 conducted in Norway. Their results confirmed that iodocarbon gases generally occur after the Chl
300 *a* maxima. Furthermore, the mean CH_3I concentration measured in the high pCO_2 treatment was
301 significantly lower (40%) than that measured in the low pCO_2 treatment during the mesocosm
302 experiment. This result is in accordance with Hopkins et al. (2010) and Webb et al. (2015) who
303 also reported that elevated pCO_2 leads to a reduction in iodocarbon concentrations, but in contrast
304 to the findings of Hopkins et al. (2013) and Webb et al. (2016) who showed that elevated pCO_2
305 does not significantly affect the iodocarbon concentrations in the mesocosms. Considering that the
306 phytoplankton species did not show significant differences in the high pCO_2 and low pCO_2
307 treatments during the experiment, this reduction in the high pCO_2 treatment was likely not caused
308 by phytoplankton. Apart from direct biological production via methyl transferase enzyme activity
309 by both phytoplankton and bacteria (Amachi et al., 2001), CH_3I is produced from the breakdown
310 of higher molecular weight iodine-containing organic matter (Fenical, 1982) through
311 photochemical reactions between organic matter and light (Richter and Wallace, 2004). Both

bacterial methyl transferase enzyme activity and photochemical reaction could be responsible for the reduction of CH_3I concentrations in the high pCO_2 treatment but further experiments are needed to verify this result.

4. Conclusions

In this study, the effects of increased levels of pCO_2 on marine DMS(P) and halocarbons release were studied in a controlled mesocosm facility. During the logarithmic growth phase, the elevated pCO_2 led to a reduction in mean DMSP-consuming bacteria (29%) and DMS concentration (28%) compared with those in the low pCO_2 treatment. In addition, a 4 d delay in DMS concentration was observed in the high pCO_2 treatment due to the effect of elevated pCO_2 and we attribute this delay in DMS concentration to the DMSP-consuming bacteria attached to *P. tricornuntum* and *T. weissflogii*. Due to the loss of main bromocarbon-producing species affected by the filtration procedure, three bromocarbons compounds measured in this study were not correlated with *P. tricornuntum* and *T. weissflogii*, and Chl *a*. Besides, elevated pCO_2 had no effect on any of the three bromocarbons. The temporal dynamics of CH_3I, combined with strong correlations with *P. tricornuntum* and *T. weissflogii*, and Chl *a*, indicate that *P. tricornuntum* and *T. weissflogii* play a critical role controlling CH_3I concentrations. In addition, the production of CH_3I was sensitive to pCO_2, with a significant increase in CH_3I concentration at higher pCO_2. However, without additional empirical measurements, it is unclear whether this decrease was caused by bacterial methyl transferase enzyme activity or by photochemical degradation at higher pCO_2.

Author contribution: Gui-Peng Yang and Kun-Shan Gao designed the experiments. Sheng-Hui Zhang, Juan Yu and Qiong-Yao Ding carried out the experiments and prepared the manuscript. Hong-Hai Zhang and Da-Wei Pan revised the paper.

334 **Acknowledgements**

335 This study was financially supported by the National Natural Science Foundation of China (Grant
336 Nos. 41320104008, 41576073 and 41830534), the National Key Research and Development
337 Program of China (Grant No. 2016YFA0601300), and AoShan Talents Program of Qingdao
338 National Laboratory for Marine Science and Technology (No. 2015 ASTP). We are thankful to
339 Minhan Dai for the nutrient data and to Bangqin Huang for the bacterial data.

340 Competing interests: The authors declare that they have no conflict of interest.

341 **References**

342 Alessandrade, M., Agnès, M., Shi, J., Pan, K., Chris, B.: Genetic and phenotypic characterization of
343 *Phaeodactylum tricornutum* (Bacillariophyceae) accessions. J. Phycol., 43, 992–1009, 2007.

344 Amachi, S., Kamagata, Y., Kanagawa, T., and Muramatsu, Y.: Bacteria mediate methylation of iodine in marine
345 and terrestrial environments, Appl. Environ. Microb., 67, 2718–2722, 2001.

346 Archer, S. D., Kimmance, S. A., Stephens, J. A., Hopkins, F. E., Bellerby, R. G. J., Schulz, K. G., Piontek, J., and
347 Engel, A.: Contrasting responses of DMS and DMSP to ocean acidification in Arctic waters, Biogeosciences,
348 10, 1893–1908, 2013.

349 Avgoustidi, V., Nightingale, P. D., Joint, I., Steinke, M., Turner, S. M., Hopkins, F. E., and Liss, P. S.: Decreased
350 marine dimethyl sulfide production under elevated CO_2 levels in mesocosm and in vitro studies, Environ.
351 Chem., 9, 399–404, 2012.

352 Bacic, M. K., Yoch, D. C.: In vivo characterization of dimethylsulfoniopropionatelyase in the fungus
353 *Fusariumlateritium*, Appl. Environ. Microbiol., 64, 106–111, 1998.

354 Boyd, P. W., Doney, S. C.: Modelling regional responses by marine pelagic ecosystems to global climate change,
355 Geophys. Res. Lett., 29, 1–4, 2002.

356 Charlson, R. J., Lovelock, J. E., Andreae, M. O., Wakeham, S. G.: Oceanic phytoplankton, atmospheric sulfur,
357 cloud albedo and climate, Nature, 326, 655–661, 1987.
358 Curson, A. R., Liu, J., Mart ńez, A. B., Green, R., Chan, Y., Carrion, O. Williams, B. T., Zhang, S. H., Yang, G. P.,
359 Page, P. C. B., Zhang, X. H., Todd, J. D.: Dimethylsulfoniopropionate biosynthesis in marine bacteria and
360 identification of the key gene in this process. Nat. Microbiol., 2, 17009, 2017.
361 Czerny, J., Schulz, K. G., Ludwig, A., and Riebesell, U.: Technical Note: A simple method for air–sea gas
362 exchange measurements in mesocosms and its application in carbon budgeting, Biogeosciences, 10,
363 1379–1390, 2013.
364 de Souza, M. P., Yoch, D. C.: Purification and characterization of dimethylsulfoniopropionatelyase from an
365 *Alcaligenes*-like dimethyl sulfide-producing marine isolate, Appl. Environ. Microbiol., 61, 21–26, 1995.
366 Doney, S. C., Fabry, V. J., Feely, R. A., and Kleypas, J. A.: Ocean acidification: the other CO_2 problem, Annu. Rev.
367 Mar. Sci., 1, 169–192, 2009.
368 Fenical, W.: Natural products chemistry in the marine environment, Science, 215, 923–928, 1982.
369 Gattuso, J. P., Gao, K., Lee, K., Rost, B., Schulz, K. G.: Approaches and tools to manipulate the carbonate
370 chemistry. In: Riebesell, U., et al. (Eds.), Guide to Best Practices in Ocean Acidification Research and Data
371 Reporting. Office for Official Publications of the European Communities, Luxembourg, pp. 41–52, 2010.
372 Gattuso, J. P., Magnan, A., Bille, R., Cheung, W. W. L., Howes, E. L., Joos, F., Allemand, D., Bopp, L., Cooley, S.
373 R., Eakin, C. M., Hoegh-Guldberg, O., Kelly, R. P., Portner, H. O., Rogers, A. D., Baxter, J. M., Laffoley, D.,
374 Osborn, D., Rankovic, A., Rochette, J., Sumaila, U. R., Treyer, S., Turley, C.: Contrasting futures for ocean
375 and society from different anthropogenic CO_2 emissions scenarios. Science, 349 (6243), aac4722, 2015.
376 Hopkins, F. E. and Archer, S. D.: Consistent increase in dimethyl sulfide (DMS) in response to high CO_2 in five
377 shipboard bioassays from contrasting NW European waters, Biogeosciences, 11, 4925–4940, 2014.

Hopkins, F. E., Kimmance, S. A., Stephens, J. A., Bellerby, R. G. J., Brussaard, C. P. D., Czerny, J., Schulz, K. G., Archer, S. D.: Response of halocarbons to ocean acidification in the Arctic, Biogeosciences, 10, 2331–2345, 2013.

Hopkins, F. E., Turner, S. M., Nightingale, P. D., Steinke, M., and Liss, P. S.: Ocean acidification and marine biogenic trace gas production, P. Natl. Acad. Sci. USA, 107, 760–765, 2010.

Huang, Y. B., Liu, X., Edward, A. L., Chen, B. Z., Li Y., Xie, Y. Y., Wu, Y. P., Gao K. S., Huang, B. Q.: Effects of increasing atmospheric CO_2 on the marine phytoplankton and bacterial metabolism during a bloom: A coastal mesocosm study, Sci. Total. Environ., 633, 618–629, 2018.

Hughes, C., Johnson, M., Utting, R., Turner, S., Malin, G., Clarke, A., and Liss, P. S.: Microbial control of bromocarbon concentrations in coastal waters of the western Antarctic Peninsula, Mar. Chem., 151, 35–46, 2013.

Jenkins, M. E., Cox, R. A., Hayman, G. D.: Kinetics of the reaction of IO radicals with HO_2 at 298 K, Chem. Phys. Lett., 177, 272–278, 1991.

Karlsson, A., Auer, N., Schulz-Bull, D., and Abrahamsson, K.: Cyanobacterial blooms in the Baltic–A source of halocarbons, Mar. Chem., 110, 129–139, 2008.

Kiene, R. P., Linn, L. J., Gonzalez, J., Moran, M. A., Bruton, J. A.: Dimethylsulfoniopropionate and methanethiol are important precursors of methionine and protein-sulfur in marine bacterioplankton, Appl. Environ. Microbiol., 65, 4549–4558, 1999.

Kiene, R. P., Linn, L. J.: The fate of dissolved dimethylsulfoniopropionate (DMSP) in seawater: tracer studies using ^{35}S-DMSP. Geochim, Cosmochim. Acta., 64, 2797–2810, 2000.

Kiene, R. P., Slezak, D.: Low dissolved DMSP concentrations in seawater revealed by smallvolume gravity filtration and dialysis sampling, Limnol. Oceanogr. Methods, 4, 80–95, 2006.

Kirkwood, M., Le Brun, N. E., Todd, J. D., Johnston, A. W. B.: The dddP gene of Roseovarius nubinhibens encodes a novel lyase that cleaves dimethylsulfoniopropionate into acrylate plus dimethyl sulfide, Microbiology, 156, 1900–1906, 2010.

Li, Y. H., Xu, J. T., Gao, K.: Light-modulated responses of growth and photosynthetic performance to ocean acidification in the model diatom Phaeodactylum tricornutum. PLoS One, 9, e96173, 2014.

Liss, P., Marandino, C. A., Dahl, E., Helmig, D., Hintsa, E. J., Hughes, C., Johnson, M., Moore, R. M., Plane, J. M. C., Quack, B., Singh, H. B., Stefels, J., von Glasow, R., and Williams, J.: Short-lived trace gases in the surface ocean and the atmosphere, in: Ocean-Atmosphere Interactions of Gases and Particles, edited by: Liss, P. and Johnson, M., 55–112, 2014.

Liu, N., Tong, S., Yi, X., Li, Y., Li, Z., Miao, H., Wang, T., Li, F., Yan, D., Huang, R., Wu, Y., Hutchins, D. A., Beardall, J., Dai, M., Gao, K.: Carbon assimilation and losses during an ocean acidification mesocosm experiment, with special reference to algal blooms, Mar. Environ. Res., 129, 229–235, 2017.

Manley, S. L., De La Cuesta, J. L. 1997. Methyl iodide production from marine phytoplankton cultures, Limnol. Oceanogr., 42, 142–147.

Orr, J. C., Fabry, V. J., Aumont, O., Bopp, L., Doney, S. C., Feely, R. A., Gnanadesikan, A., Gruber, N., Ishida, A., Joos, F., Key, R. M., Lindsay, K., Maier-Reimer, E., Matear. R., Monfray, P., Mouchet, A., Najjar, R. G., Plattner, G. K., Rodgers, K. B., Sabine, C. L., Sarmiento, J. L., Schlitzer, R., Slater, R. D., Totterdell, I. J., Weirig, M. F., Yamanaka, Y., Yool, A.: Anthropogenic ocean acidification over the twenty first century and its impact on calcifying organisms, Nature, 437, 681–686, 2005.

Porra, R. J.: The chequered history of the development and use of simultaneous equations for the accurate determination of chlorophylls a and b. Photosynth. Res., 73, 149–156, 2002.

Porter, K. G., Feig, Y. S.: DAPI for identifying and counting aquatic microflora. Limnol. Oceanogr., 25, 946–948,

1980.

Quinn, P. K., Bates, T. S.: The case against climate regulation via oceanic phytoplankton sulphur emissions, Nature, 480, 51–56, 2011.

Raina, J. B., Tapiolas, D., Motti, C. A., Foret, S., Seemann, T., Tebben, J.: Isolation of an antimicrobial compound produced by bacteria associated with reef-building corals. PeerJ, 4, e2275, 2016

Richter, U., Wallace, D. W. R.: Production of methyl iodide in the tropical Atlantic Ocean, Geophys. Res. Lett., 31, L23S03, doi:10.1029/2004GL020779, 2004.

Riebesell, U., Czerny, J., von Brckel, K., Boxhammer, T., Büdenbender, J., Deckelnick, M., Fischer, M., Hoffmann, Krug, S. A., Lentz, U., Ludwig, A., Muche, R., Schulz, K. G.: Technical Note: a mobile sea-going mesocosm system-new opportunities for ocean change research, Biogeosciences, 10, 1835–1847, 2013.

Roy, R., Pratihary, A., Narvenkar, G., Mochemadkar, S., Gauns, M., and Naqvi, S. W. A.: The relationship between volatile halocarbons and phytoplankton pigments during a *Trichodesmium* bloom in the coastal eastern Arabian Sea, Estuar. Coast. Shelf Sci., 95, 110–118, 2011.

Simó, R., Archer, S. D., Pedros-Alio, C., Gilpin, L., and StelfoxWiddicombe, C. E.: Coupled dynamics of dimethylsulfoniopropionate and dimethylsulfide cycling and the microbial food web in surface waters of the North Atlantic, Limnol. Oceanogr., 47, 53–61, 2002.

Simó, R., Vila-Costa, M., Alonso-Sáez, L., Cardelús, C., Guadayol, Ó., Vázquez-Dominguez, E., and Gasol, J. M.: Annual DMSP contribution to S and C fluxes through phytoplankton and bacterioplankton in a NW Mediterranean coastal site, Aquat. Microb. Ecol., 57, 43–55, 2009.

Stefels, J., Dijkhuizen, L.: Characteristics of DMSP-lyase in *Phaeocystis*sp. (Prymnesiophyceae), Mar. Ecol. Prog. Ser., 131, 307–313, 1996.

Stefels, J., Steink, M., Turner, S., Malin, G., Belviso, S.: Environmental constraints on the production of the

444 climatically active gas dimethylsulphide (DMS) and implications for ecosystem modelling, Biogeochemistry,
445 83, 245–275, 2007.

446 Steinke, M., Kirst, G. O.: Enzymatic cleavage of dimethylsulfoniopropionate (DMSP) in cell-free extracts of the
447 marine macroalga *Enteromorphaclathrata* (Roth) Grev (Ulvales, Chlorophyta), J. Exp. Mar. Biol. Ecol., 201,
448 73–85, 1996.

449 Sugie, K., Yoshimura, T.: Effects of high CO_2 levels on the ecophysiology of the diatom *Thalassiosira weissflogii*
450 differ depending on the iron nutritional status. ICES J. Mar. Sci., 73, 680–692, 2016.

451 Todd, J. D., Rogers, R., Li, Y.G., Wexler, M., Bond, P. L., Sun, L., Cruson, A. R. J., Malin, G., Steinke, M.,
452 Johnston, A. W. B.: Structural and regulatory genes required to make the gas dimethyl sulfide in bacteria,
453 Science, 315, 666–669, 2007.

454 Visscher, P. T., Quist, P., van Gemerden, H.: Methylated sulfur compounds in microbial mats: in situ
455 concentrations and metabolism by a colorless sulfur bacterium. Appl. environ. Microbiol., 57, 1758–1763,
456 1991.

457 Vogt, M., Steinke, M., Turner, S. M., Paulino, A., Meyerhöfer, M., Riebesell, U., LeQuéré, C., and Liss, P. S.:
458 Dynamics of dimethylsulphoniopropionate and dimethylsulphide under different CO_2 concentrations during
459 a mesocosm experiment, Biogeosciences, 5, 407–419, 2008.

460 Webb, A. L., Leedham-Elvidge, E., Hughes, C., Hopkins, F. E., Malin, G., Bach, L. T., Schulz, K., Crawfurd, K.,
461 Brussaard, C. P. D., Stuhr, A., Riebesell, U., Liss, P. S.: Effect of ocean acidification and elevated *f*CO2 on
462 trace gas production by a Baltic Sea summer phytoplankton community, Biogeosciences, 13, 4595–4613,
463 2016.

464 Webb, A. L., Malin, G., Hopkins, F. E., Ho, K. L., Riebesell, U., Schulz, K., Larsen, A., and Liss, P.: Ocean
465 acidification has different effects on the production of dimethylsulphide and dimethylsulphoniopropionate

measured in cultures of Emiliania huxleyi RCC1229 and mesocosm study: a comparison of laboratory monocultures and community interactions, Environ. Chem., 13, EN14268, doi:10.1071/EN14268, 2015.

Wingenter, O. W., Haase, K. B., Zeigler, M., Blake, D. R., Rowland, F. S., Sive, B. C., Paulino, A., Thyrhaug, R., Larsen, A., Schulz K., Meyerhofer, M., Riebesell, U.: Unexpected consequences of increasing CO_2 and ocean acidity on marine production of DMS and CH2ClI: Potential climate impacts, Geophys. Res. Lett., 34, L05710, 2007.

Xing, T., Gao, K., Beardall, J.: Response of growth and photosynthesis of *Emiliania huxleyi* to visible and UV irradiances under different light regimes. Photochem. Photobiol., 91, 343–349, 2015.

Yang, G. P., Lu, X. L., Song, G. S., Wang, X. M.: Purge-and-trap gas chromatography method for analysis of methyl chloride and methyl bromide in seawater. Chin. J. Anal. Chem., 38 (5), 719–722, 2010.

Yost, D. M., Mitchelmore, C. L.: Dimethylsulfoniopropionate (DMSP) lyase activity in different strains of the symbiotic alga Symbiodinium microadriaticum. Mar. Ecol. Prog. Ser., 386, 61–70, 2009.

Yuan, D., Yang, G. P., He, Zhen.,: Spatio-temporal distributions of chlorofluorocarbons and methyl iodide in the Changjiang (Yangtze River) estuary and its adjacent marine area, Mar. Pollut. Bull., 103 (1-2), 247–259, 2016.

Zhang, S.H., Yang, G.P., Zhang, H.H., Yang, J.: Spatial variation of biogenic sulfur in the south Yellow Sea and the East China Sea during summer and its contribution to atmospheric sulfate aerosol. Sci. Total Environ., 488–489, 157–167, 2014.

Figure captions

Fig. 1 Temporal development of pH in the high pCO_2 (1,000 µatm, solid squares) and low pCO_2 (400 µatm, white squares) mesocosms. Data are mean ± standard deviation, n = 3 (triplicate independent mesocosm bags) (Origin 8.0).

Fig. 2 Temporal development in dimethylsulfide (DMS), dimethylsulfoniopropionate (DMSP) and DMSP-consuming bacteria concentrations in the high pCO_2 (1,000 µatm, black squares) and low pCO_2 (400 µatm, white squares) mesocosms. Data are mean ± standard deviation, n = 3 (triplicate independent mesocosm bags).

Fig. 3 Temporal development in bromodichloromethane ($CHBrCl_2$), methyl bromide (CH_3Br), dibromomethane (CH_2Br_2), iodomethane (CH_3I) concentrations in the high pCO_2 (1,000 µatm, black squares) and low pCO_2 (400 µatm, white squares) mesocosms. Data are mean ± standard deviation, n = 3 (triplicate independent mesocosm bags).

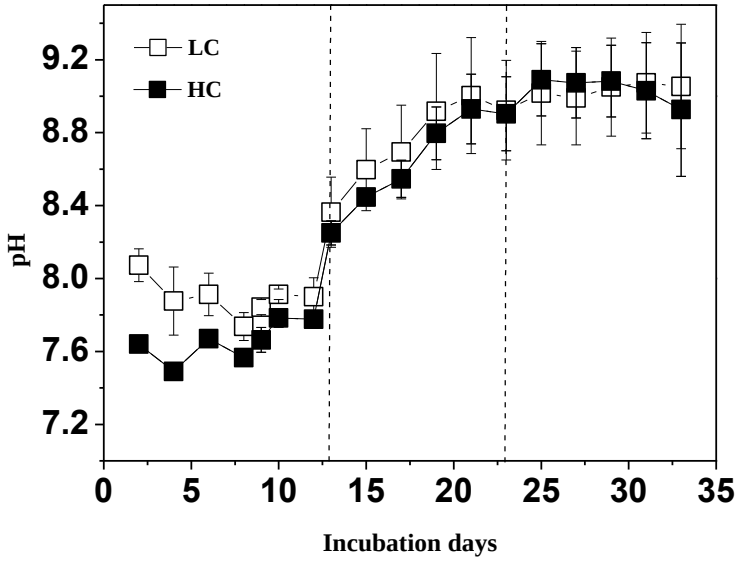

499

500 **Fig. 1.** Temporal changes of pH in the high pCO_2 (1,000 μatm, solid squares) and low pCO_2 (400 μatm, white

501 squares) mesocosms. Data are mean ± standard deviation, n = 3 (triplicate independent mesocosm bags) (Origin

502 8.0).

503

504

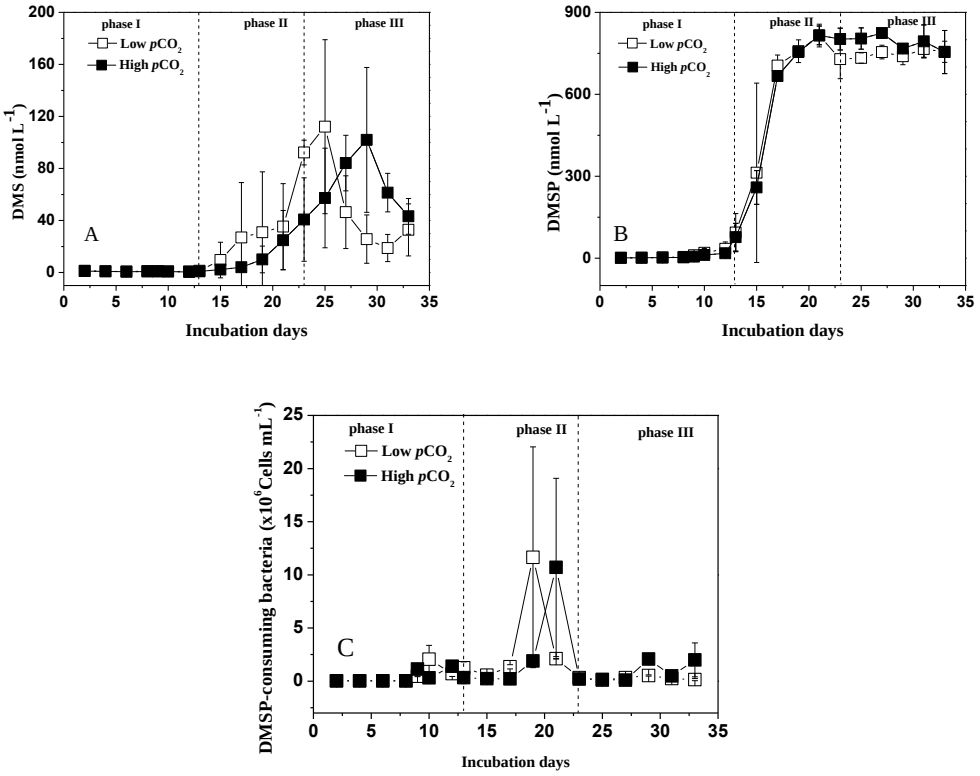

505

506

507 **Fig. 2** Temporal changes in dimethylsulfide (DMS), dimethylsulfoniopropionate (DMSP), DMSP-consuming

508 bacteria concentrations in the high pCO_2 (1,000 μatm, black squares) and low pCO_2 (400 μatm, white squares)

509 mesocosms. Data are mean ± standard deviation, n = 3 (triplicate independent mesocosm bags) (Origin 8.0).

510

511

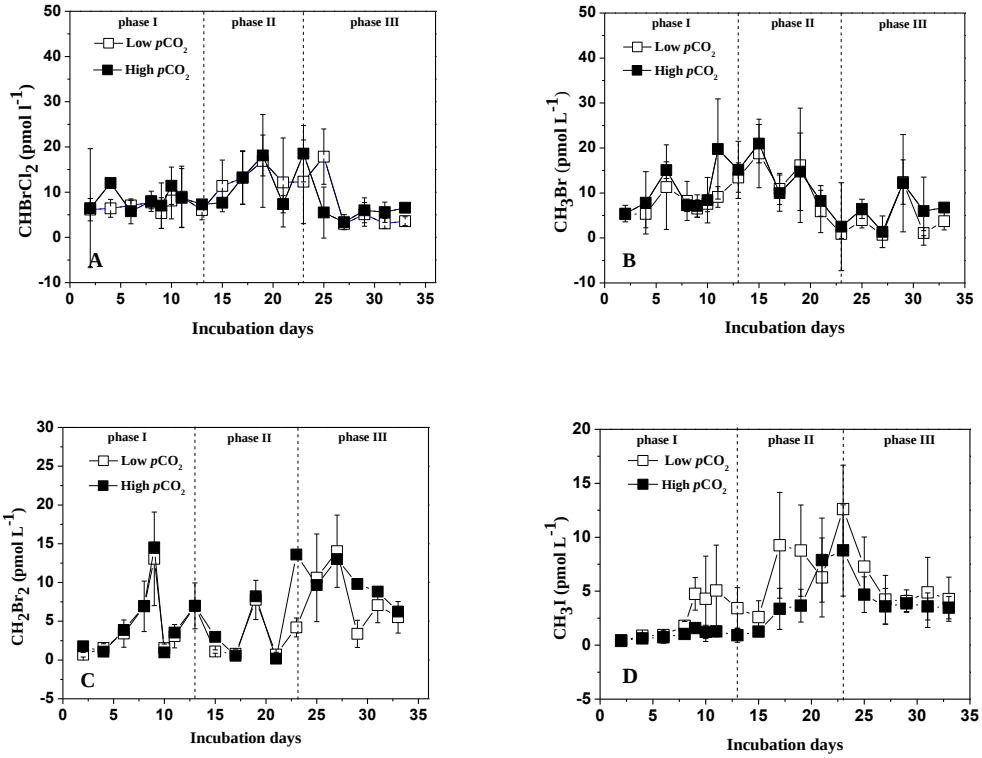

512

513

514 **Fig. 3** Temporal changes in bromodichloromethane ($CHBrCl_2$), methyl bromide (CH_3Br), dibromomethane

515 (CH_2Br_2), iodomethane (CH_3I) concentrations in the high pCO_2 (1,000 µatm, black squares) and low pCO_2 (400

516 µatm, white squares) mesocosms. Data are mean ± standard deviation, n = 3 (triplicate independent mesocosm

517 bags) (Origin 8.0).

518

519 **Table 1**. Dissolved inorganic carbon (DIC), pH, pCO_2 and nutrient concentrations in the mesocosm experiments. "-" means that the values were below the detection limit.

		pH	DIC ($\mu mol\ kg^{-1}$)	pCO_2 (μatm)	$NO_3^-+NO_2^-$ ($\mu mol\ L^{-1}$)	NH_4^+ ($\mu mol\ L^{-1}$)	PO_4^{3-} ($\mu mol\ L^{-1}$)	SiO_3^{2-} ($\mu mol\ L^{-1}$)
day 0	Low pCO_2	8.0±0.1	2181±29	1170~1284	52~56	19~23	2.6±0.2	38~40
	High pCO_2	7.5±0.1	2333±34	340~413	51~55	19~23	2.5±0.2	38~39
PhaseI	Low pCO_2	7.9~8.4	1825~2178	373~888	15~52	1.6~20	0.5~2.6	31~38
	High pCO_2	7.4~8.2	2029~2338	1295~1396	47~54	0.2~21	0.7~2.5	34~39
Phase II	Low pCO_2	8.4~8.5	1706~1745	46~749	-~ 15.9	-	0.1~0.5	10~24
	High pCO_2	8.4~8.6	1740~1891	59~1164	1.1~25	-	-~0.1	29~30
Phase III	Low pCO_2	8.5~8.8	1673~1706	30~43	-	-	-	10~16
	High pCO_2	8.6~8.7	1616~1740	34~110	-	-	-~0.3	24~25

520 **Table 2**. Correlation between dimethylsulfide (DMS), dimethylsulfoniopropionate (DMSP), chlorophyll a (Chl *a*), bromodichloromethane ($CHBrCl_2$), methyl bromide (CH_3Br),

521 dibromomethane (CH_2Br_2), iodomethane (CH_3I), DMSP-consuming bacteria, *Thalassiosira weissflogii* (*T. weissflogii*) and *Phaeodactylum tricornutum* (*P. tricornutum*) concentrations in the

522 low pCO_2 treatments.

	DMS	DMSP	Chl *a*	$CHBrCl_2$	CH_3Br	CH_2Br_2	CH_3I	DMSP-consuming bacteria	*T. weissflogii*	*P. tricornutum*
DMS	1									
DMSP	0.701**	1								
Chl *a*	0.597**	0.792**	1							
$CHBrCl_2$	0.526	0.280	0.559	1						
CH_3Br	-0.413	-0.230	0.196	0.313	1					
CH_2Br_2	0.310	0.180	0.001	-0.136	-0.308	1				
CH_3I	0.694**	0.654**	0.717**	0.596*	-0.151	0.129	1			
DMSP-consuming bacteria	0.643**	0.520*	0.522*	0.394	-0.268	-0.038	0.762**	1		
T. weissflogii	0.410	0.617**	0.899**	0.301	0.322	0.028	0.680**	0.399	1	
P. tricornutum	0.560*	0.961**	0.821**	0.528	-0.032	0.162	0.588**	0.334	0.685**	1

523 *. Correlation is significant at the 0.05 level (2-tailed).

524 **. Correlation is significant at the 0.01 level (2-tailed).

525

526

527

528

529

530 **Table 3**. Correlation between dimethylsulfide (DMS), dimethylsulfoniopropionate (DMSP), chlorophyll a (Chl *a*), bromodichloromethane ($CHBrCl_2$), methyl bromide (CH_3Br),

531 dibromomethane (CH_2Br_2), iodomethane (CH_3I), DMSP-consuming bacteria, *Thalassiosira weissflogii* (*T. weissflogii*) and *Phaeodactylum tricornutum* (*P. tricornutum*) concentrations in the

532 high pCO_2 treatments.

	DMS	DMSP	Chl *a*	$CHBrCl_2$	CH_3Br	CH_2Br_2	CH_3I	DMSP-consuming bacteria	*T. weissflogii*	*P. tricornutum*
DMS	1									
DMSP	0.752**	1								
Chl *a*	0.318*	0.738**	1							
$CHBrCl_2$	0.324	0.094	0.326	1						
CH_3Br	-0.410	-0.349	0.065	0.076	1					
CH_2Br_2	0.540*	0.352	0.142	0.233	-0.377	1				
CH_3I	0.694**	0.816**	0.741**	0.690*	-0.407	0.316	1			
DMSP-consuming bacteria	0.544*	0.522	0.549*	0.532	-0.311	0.368	0.851*	1		
T. weissflogii	0.355	0.743**	0.930**	0.304	0.076	0.233	0.690**	0.567	1	
P. tricornutum	0.635**	0.954**	0.803**	0.143	-0.257	0.267	0.834**	0.559	0.820**	1

533 *. Correlation is significant at the 0.05 level (2-tailed).

534 **. Correlation is significant at the 0.01 level (2-tailed).

535